

# A dual-band rectangular shape incorporated into circular patch antenna for 2.4/5 GHz wireless local area network applications

Suthasinee Lamultree<sup>1</sup>, Nattakarn Somsanook<sup>1</sup>, Wararak Narkkoht<sup>1</sup>, Chuwong Phongcharoenpanich<sup>2</sup>

<sup>1</sup>Department of Electronics and Telecommunication Engineering, Faculty of Engineering, Rajamangala University of Technology Isan Khonkaen Campus, Khonkaen, Thailand

<sup>2</sup>Department of Telecommunications Engineering, School of Engineering, King Mongkut's Institute of Technology Ladkrabang, Bangkok, Thailand

## Article Info

### Article history:

Received Jul 31, 2024

Revised Oct 1, 2024

Accepted Oct 18, 2024

### Keywords:

2.4/5 wireless local area network

Circular shape

Dual-band antenna

Inverted U-slots

Omnidirectional antenna

Patch antenna

Rectangular shape

## ABSTRACT

This research exhibits a design of a dual-band patch antenna (DBPA) implemented by a rectangular shape incorporated into a circular patch together with a pair of half-wavelength inverted U-slots (HWIUSs) with the single feed for 2.4/5 GHz wireless local area network (WLAN) applications. For this work, the HWIUSs are key in designing a dual-band antenna. The DBPA is fed by a 50-Ohm microstrip line, printed on a copper layer overlaid on an FR4 substrate with a relative permittivity of 4.3 and height of 1.6 mm, while the bottom layer is backed by a partial ground plane. An antenna prototype with a dimension of  $0.384\lambda_L \times 0.304\lambda_L \times 0.013\lambda_L$  was contrived and admeasured to verify the simulation. The measurement provides a nearly omnidirectional pattern with a 2.55 and 3.3 dBi peak gain covering a dual-band 10 dB return loss bandwidth of 15% (2.4–2.8 GHz) and 20% (4.96–5.86 GHz), respectively. Noticeably, simulated  $|S_{11}|$  and radiation patterns are reasonable following experimental results showing its potential in 2.4/5 GHz WLAN services.

This is an open access article under the [CC BY-SA](https://creativecommons.org/licenses/by-sa/4.0/) license.



## Corresponding Author:

Suthasinee Lamultree

Faculty of Engineering, Rajamangala University of Technology Isan Khonkaen Campus

Khonkaen, 40000, Thailand

Email: suthasinee.la@rmuti.ac.th

## 1. INTRODUCTION

With the rise of mobile internet, internet of things (IoT), and Bluetooth, the router/access point antenna has become a key device in wireless local area network (WLAN) systems to accommodate the increasing requirement for connecting mobile terminals for higher transmission rates and security. For the broad area coverage, omnidirectional radiation in the azimuthal plane is suitably desired for the router antennas [1]-[3]. Wireless fidelity (Wi-Fi) has transformed into the standard for WLAN communications in the 2.4 and 5 GHz ISM bands, with the frequency ranges from 2.4 to 2.485 GHz as well as 5.150–5.350 GHz, 5.470–5.725 GHz, and 5.725–5.850 GHz [4]-[7]. For system mobility and expedience, a single antenna simultaneously overspreads the multi-variant bands is preferred [8]-[16] as it is necessary to integrate the multi-functional operation on a single antenna without handling other devices like a duplexer, or multi-feeding network [17], [18]. Therefore, dual-band antennas are recommended to dominate the 2.4 and 5 GHz WLAN bands [7], [19]-[21]. Assorted methods have been launched in the past years to design dual-, and multi-band antennas that are empowered to enclose the current standards.

From the literature, the compact, dual-band operation, an omnidirectional pattern antenna is presented in [1], [7]. A couple of feed with two parasitic metals inside the antenna box is introduced to achieve two transition band operations in [1]; nonetheless, the antenna gain is not high. Research by Song *et al.* [7], an

omnidirectional WLAN loop-slot antenna with common-mode current (CMC) is reported to cover dual-band operation with improving real gain. Other ways to acquire an omnidirectional pattern antenna with high gain, a cavity and slot-dipole hybrid structure with array scalability are proposed in [2], and a compact monopole antenna using the meander line method in a horizontal shape with different lengths is introduced in [3]. Otherwise, the antennas in [2] and [3] cover only a single band of 2.4 GHz WLAN applications. According to Hossain *et al.* [5], a simple square loop monopole radiating patch is integrated into a bandpass filter (BPF) for a single band 5 GHz WLAN. A single feed 4G/5G three-band antenna is proposed in [6], it consists of a dual-band (2.4/5.5 GHz) franklin monopole antenna together with stub in a partial ground, 5G rectangular patch antenna (28 GHz) and modified compact microstrip resonant cell (CMRC) low-pass filter (LPF) between antenna parts which is complexity in the design process. Research by Khan *et al.* [9], a defected ground structure (DGS) slotted double patch antenna is proposed for WLAN and 5G applications; the dimension of the antenna is small, however, its structures kind of added complexity. According to Seko and Correra [8], a compact dimension with the technique of multi-mode radiators is presented for the portable WLAN application, however, the antenna gain is quite low. Likewise, Ghouse *et al.* [16] present a compact dual-band antenna using characteristic mode theory to generate two variant resonant modes. As well as the complicated design process of the metamaterial-fractal-defected ground structure used in [11], and the metamaterial antenna design for dual-band 2.4/5 GHz WLAN [20]. Chang and Liu [13] present a low-profile and miniaturized dual-band patch antenna (DBPA) by applying magnetic coupling to enhance the impedance bandwidth. Moreover, a tri-band antenna comprised of an inner loop, a parasitic strip, and three-sided vertical ground together with tuning stubs is introduced in [14], which is fairly complicated in the design process. The antenna in [15] suggests the array  $2 \times 2$  dual band 28/38 GHz multiple-input multiple-output (MIMO) antenna by adding slots. The technique of multi-mode radiators is used to achieve multi-band operation it comes up with multi-excitation, mutual coupling, isolation, and a more complicated structure in [21]. In addition, the multi-ports, complex structure of  $4 \times 4$  MIMO operating covered two distinct -6 dB bandwidths is presented by using the half-mode patch and parasitic half-mode patch excited through electric coupling [22].

This work aims to present the design of a dual-band antenna for 2.4/5 GHz WLAN, the single-fed, uncomplicated geometry, cost-effectiveness, two-transmission band antenna is performed to cover 2.4–2.485 GHz as well as 5.150–5.850 GHz. The significant contributions to this work are as:

- The single antenna is capable to operate covered the two-transition band over WLAN applications;
- The antenna radiates an omnidirectional pattern with a good gain over the 2.4/5 GHz WLAN applications;
- By introducing the half-wavelength inverted U-slots (HWIUSs), a wideband antenna is transformed into a dual-band antenna without digressing the radiation property;
- Only a single feed is required through the microstrip line.

The organization of this article is as: the introduction is provided in section 1. Then, the procedure specifically designed is reported the antenna model, the evolution of the DBPA, and the initial formulas are revealed in section 2. The antenna prototype, numerical and measured results are discussed in section 3. Finally, the conclusion is addressed in section 4.

## 2. PROCEDURE SPECIFICALLY DESIGNED

### 2.1. Design layout

Figure 1 depicts the layout of the DBPA. The antenna geometry consists of a rectangular patch of width  $w_r$  and length  $l_r$  incorporated into a circular shape loaded with a pair of HWIUSs of lengths  $l_{u1}$ ,  $l_{u2}$ ,  $l_{u3}$  and small width of 0.5 mm-slot printed on top layer copper as shown in Figure 1(a); where  $h_r$  is denoted the height of rectangular shaped above the bottom of the circular patch. At the back side, there is a partial ground plane of length  $l_g$  and width  $w_g$ , where  $w_g$  equals  $w$  as shown in Figure 1(b). The proposed antenna for 2.4/5 GHz WLAN applications is modeled using the FR4 substrate having thickness  $h$  (as shown in Figure 1(c)) of 1.6 mm, relative permittivity of 4.3, and loss tangent ( $\tan \delta$ ) of 0.02, where the overall substrate dimensions are  $l \times w \times h$  (the values  $48 \times 38 \times 0.16$  mm<sup>3</sup>). This proposed antenna is excited through a 50-Ohm microstrip line of length  $l_f$  and width of  $w_f$  to deliver maximum power to the DBPA. The process of designing the DBPA is performed using CST Microwave Studio [23]. To obtain the acceptable impedance characteristic ( $|S_{11}| < -10$  dB) and radiation performance, antenna parameters are adjusted and selected for the appropriate choice. Subsequently, the final set of the design parameters is reported in Table 1.

### 2.2. Evolution of the design antenna

The stepwise modification of the designed antenna to the final DBPA is exposed to view in three successive stages as portrayed in Figure 2. The circular patch of radius  $r$  (value 13 mm) fed by a 50-Ohm microstrip line and backed by a partial ground plane (Ant#1 in Figure 2(a)) is firstly designed, by using (1) [24], where  $r$  is the radius in cm, to resonate at 2.45 GHz.

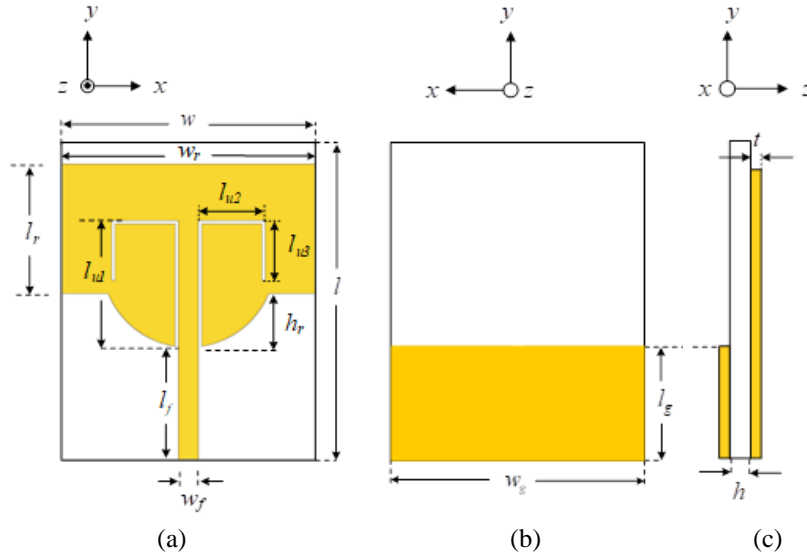


Figure 1. Layout of the DBPA: (a) top view, (b) rear view, and (c) side view

Table 1. Selected best values for parameters of the DBPA

Variable	Parameter	Physical size (mm)
$w$	Width of the substrate	38
$l$	Length of the substrate	48
$r$	Radius of the circular patch	13
$l_r$	Length of a rectangular patch	19.5
$w_r$	Width of a rectangular patch	38
$h_r$	Height of the rectangular patch above the bottom of the circular patch	8
$l_{u1}$	The vertical long length of HWIUS	19
$l_{u2}$	The horizontal length of HWIUS	10
$l_{u3}$	Vertical short length of HWIUS	9
$t$	Thickness of the copper layer	0.035
$l_f$	Length of the feeding microstrip line	17
$w_f$	Width of the feeding microstrip line	3
$l_g$	Length of the ground plane	17
$w_g$	Width of the ground plane	38
$h$	The thickness of the substrate	1.6

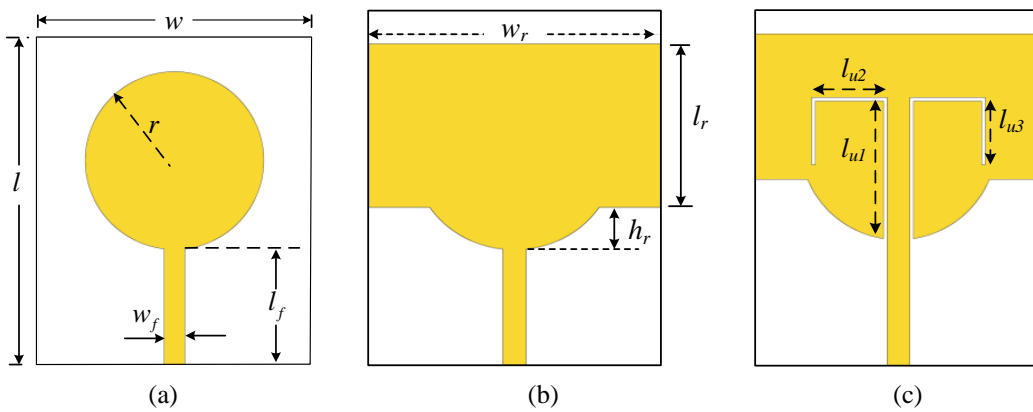


Figure 2. The developed antenna: (a) Ant#1, (b) Ant#2, and (c) proposed DBPA

$$f_r = \frac{72}{2.25r} \text{ GHz} \tag{1}$$

where  $f_r$  is the resonance frequency.

Meanwhile, the width  $w_f$  of 3 mm and length  $l_f$  of 17 mm are computed for a 50-Ohm impedance using (2), (3) [25]:

$$w_f = \frac{2h}{\pi} \left\{ \left( \frac{60\pi^2}{Z_0\sqrt{\epsilon_r}} \right) - 1 - \ln \left( \frac{120\pi^2}{Z_0\sqrt{\epsilon_r}} - 1 \right) + \frac{\epsilon_r - 1}{2\epsilon_r} \left( \ln \left( \frac{60\pi^2}{Z_0\sqrt{\epsilon_r}} - 1 \right) + 0.39 - \frac{0.61}{\epsilon_r} \right) \right\} \quad (2)$$

$$l_f = \frac{\lambda_g}{4} \quad (3)$$

where  $\lambda_g$  is the guide wavelength. In the second stage, the rectangular patch of length  $l_r$  and width  $w_r$  is inserted into the circular patch (Ant# 2) making the antenna dimension larger than the Ant#1 as depicted in Figure 2(b) the length  $l_r$  and width  $w_r$  are designed by considering the fringing effect as (4)-(6) [25]:

$$w_r = \frac{c}{2f_r} \sqrt{\frac{2}{\epsilon_r + 1}} \quad (4)$$

$$l_r = \frac{c}{2f_r\sqrt{\epsilon_{reff}}} - 0.824h \left[ \frac{(\epsilon_{reff} + 0.3)(w_r + 0.264h)}{(\epsilon_{reff} - 0.258)(w_r + 0.8h)} \right] \quad (5)$$

where  $\epsilon_{reff}$  is an effective dielectric constant.

$$\epsilon_{reff} = \frac{\epsilon_r + 1}{2} + \frac{\epsilon_r - 1}{2} \sqrt{1 + \frac{12h}{w_r}} \quad (6)$$

In the final phase of the design, a pair of HWIUSs is integrated into the radiating patch, as illustrated in Figure 2(c). The combined length of  $l_{u1}$ ,  $l_{u2}$ , and  $l_{u3}$  is approximately half of the 4 GHz wavelength (38 mm), enabling the transition from wideband to dual-band operation. Ant #1 exhibits an omnidirectional radiation pattern with a gain of 2.19 dBi and a return loss of 10 dB across the frequency range of 2.26-6.77 GHz, as shown in Figures 3 and 4(a).

For Ant #2, an initial length ( $l_r$ ) of 29.5 mm and a width ( $w_r$ ) of 38 mm were used. The length  $l_r$  was subsequently shortened from the bottom up to improve the  $|S_{11}|$ , while the width remained fixed. This adjustment also raised the height ( $h_r$ ) above the lower edge of the circular patch to optimize impedance matching. Ant #2's larger electrical size results in a deeper  $|S_{11}|$  compared to Ant #1 and shifts the resonance frequency downward, producing an omnidirectional pattern with a gain of 2.38 dBi and a return loss of 10 dB across 2.03-4.91 GHz, as depicted in Figures 3 and 4(b). The final design of the proposed DBPA supports an omnidirectional pattern across two bandwidths: 2.16-2.85 GHz and 4.8-5.96 GHz, with maximum gains of 2.5 dBi at 2.45 GHz and 2.66 dBi at 5.5 GHz, as shown in Figures 3 and 4(c).

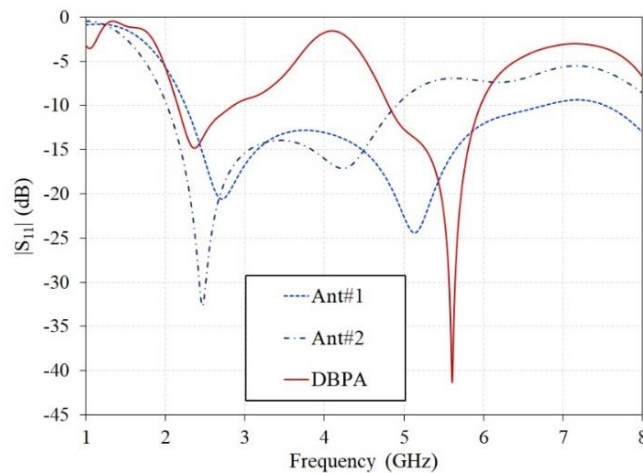


Figure 3. Comparing simulated  $|S_{11}|$  of the developed antenna

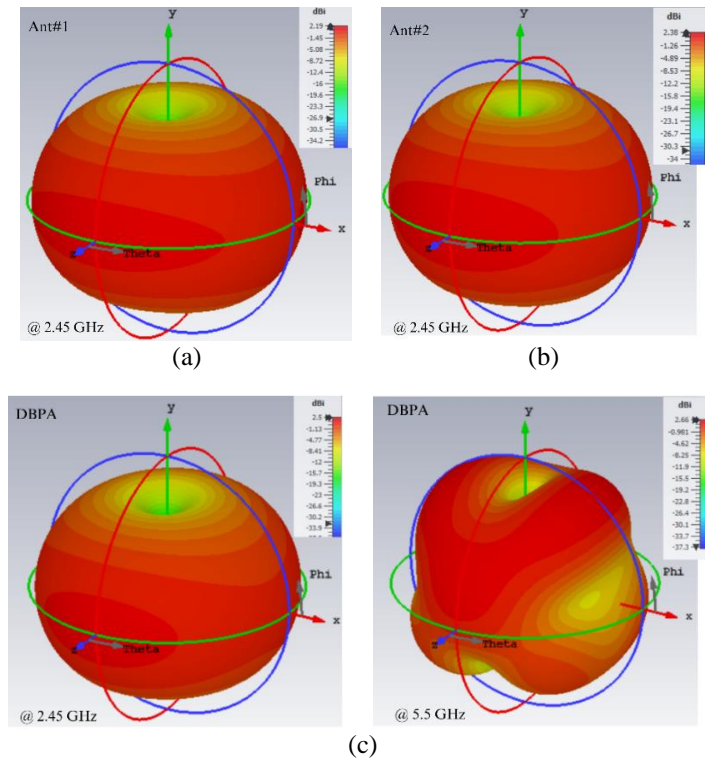


Figure 4. 3D radiation pattern of (a) Ant#1, (b) Ant#2, and (c) DBPA

Figure 5 illustrates the impact of  $h_r$  on  $|S_{11}|$ . Adding a rectangular patch over the circular patch (with  $h_r$  of 0 mm and  $l_r$  of 29.5 mm) results in a degradation of  $|S_{11}|$ . In contrast to shortening  $l_r$ , increasing  $h_r$  enhances  $|S_{11}|$  at lower frequencies and expands the bandwidth. Accordingly,  $l_r$  of 19.5 mm and  $h_r$  of 8 mm were selected for optimal  $|S_{11}|$  and to facilitate dual-band operation.

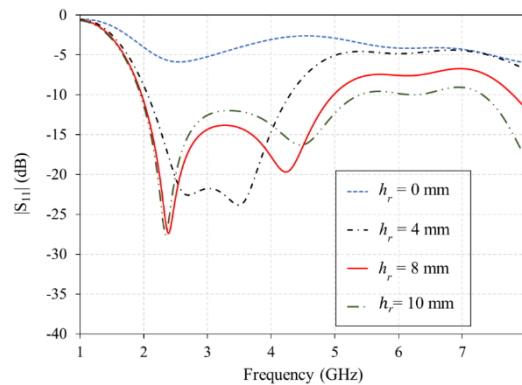
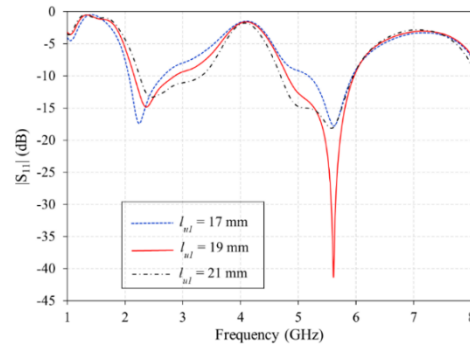
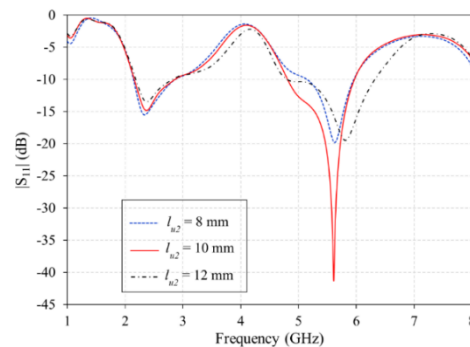


Figure 5. The effect of  $h_r$  on the  $|S_{11}|$

Subsequently, a pair of HWIUSs was added to the radiating patch to achieve dual-band performance. The effects of  $l_{u1}$  and  $l_{u2}$  on  $|S_{11}|$  are analyzed in Figures 6 and 7. In Figure 6,  $l_{u1}$  varies between 17, 19, and 21 mm, while  $l_{u2}$  remains fixed at 10 mm, and  $l_{u3}$  adjusts to maintain a total HWIUS length of 38 mm. Increasing  $l_{u1}$  leads to a shift of the lower band resonance frequency higher; while enhancing bandwidth at the upper band. Among the variations of  $l_{u1}$ , the 19 mm length offers the best  $|S_{11}|$  performance for both bands; therefore, it was selected for further examination of different  $l_{u2}$  values, as shown in Figure 7. Changes in  $l_{u2}$  primarily affect  $|S_{11}|$  at the upper band, where longer  $l_{u2}$  results in wider bandwidth and a slight frequency shift upward. Of the three options for  $l_{u2}$  (8, 10, and 12 mm), 10 mm was chosen as it delivers a 10 dB return loss over the 2.4/5 GHz wide area network (WAN) bandwidths and provides an improved  $|S_{11}|$  in the upper band.

Figure 6. The effect of  $l_{u1}$  on the  $|S_{11}|$ Figure 7. The effect of  $l_{u2}$  on the  $|S_{11}|$ 

### 3. RESULTS AND DISCUSSION

To insist on the numerical outcomes, a prototype of DBPA was fabricated on an FR4 substrate with a relative permittivity of 4.3 following the designed dimensions in Table 1 as shown in Figures 8(a) and (b) for the top and the rear views, respectively. The DBPA prototype was connected to a coaxial feeding port via a 50-ohm subminiature version A connector. Using an E5063A network analyzer as in Figure 8(c), the  $|S_{11}|$ , 2D-radiation pattern, and gain of the proposed DBPA are tested. Figure 9 depicts the simulated and tested  $|S_{11}|$  and antenna gains. Visibly, both sets pay attention to a similar trend, and the most consistent simulated and tested values do not drift much from each other. The variance was likely from a minor dissimilarity in the simulation and measurement setup: a 50- Ohm subminiature version A connector in the tested setup was not considered in the simulation. We want to emphasize only the simulated feature of the antenna itself, not other parts, and to minimize the time-consuming process. They come up with the -10 dB  $|S_{11}|$  covering the two bandwidths of WLAN applications of 2.16–2.85 GHz (27.8%), 4.8–5.96 GHz (21.5%) for the simulation, and 2.4–2.8 GHz (15%), 4.96–5.86 GHz (20%) for the measurement.

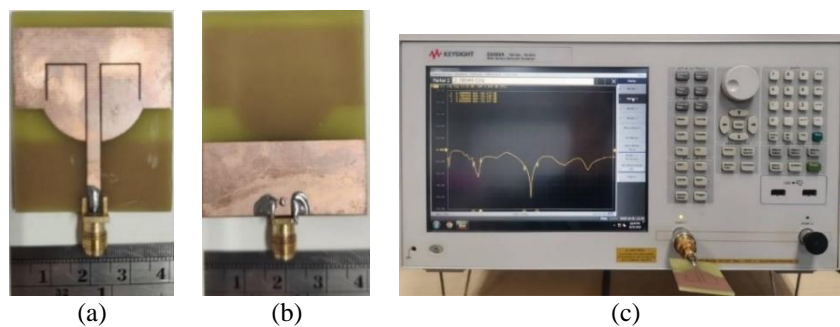


Figure 8. The DBPA prototype: (a) top view, (b) rear view, and (c) measurement

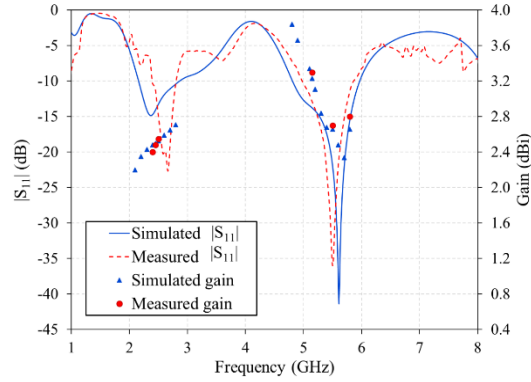


Figure 9. Comparing simulated and measured  $|S_{11}|$  and gain of the proposed DBPA

Besides the  $|S_{11}|$ , the 2D radiation pattern in  $xz$ - and  $yz$ -planes is also examined at the center operating frequencies of 2.45 and 5.5 GHz as plotted in normalized scale as in Figures 10 and 11. In the experimental setup, two identical DBPAs were used to transmit and receive antennas. Visibly, the experimental radiation patterns follow the same trend and are sensibly accepted with the simulated results. This proposed DBPA displays an omnidirectional pattern in the  $xz$ -plane, as seen in Figure 10(a), and a figure-eight pattern in the  $yz$ -plane, as depicted in Figure 10(b). Similarly, it presents a nearly omnidirectional pattern in the  $xz$ -plane and like a figure-eight pattern in the  $yz$ -plane as shown in Figures 11(a) and (b), respectively. The DBPA achieves linear polarization with peak simulated gains of 2.5 dBi at 2.45 GHz and 2.66 dBi at 5.5 GHz, along with tested gains of 2.48 dBi and 2.7 dBi at those respective frequencies as seen in Figure 9.

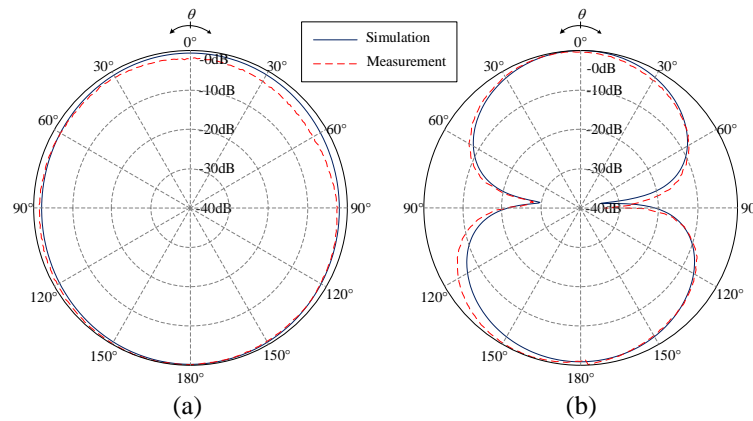


Figure 10. Simulated and measured radiation patterns at 2.45 GHz: (a)  $xz$ -plane and (b)  $yz$ -plane

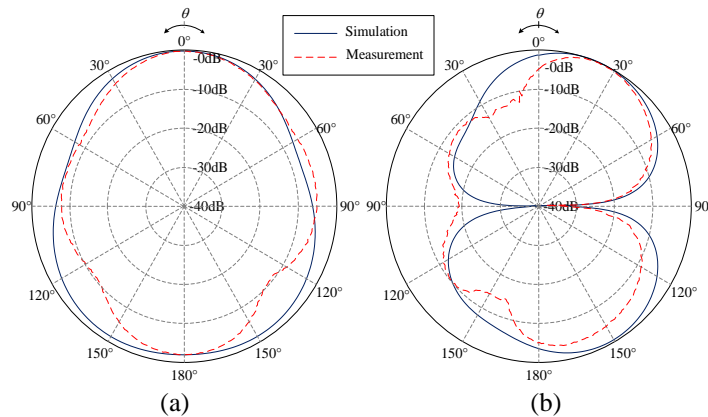


Figure 11. Simulated and measured radiation patterns at 5.5 GHz: (a)  $xz$ -plane and (b)  $yz$ -plane

Furthermore, the comparison between the proposed antenna and other designs in references is shown in Table 2. With unbiased comparison, i.e., the normalized dimension of the antenna— $\lambda_L$ , representing the free-space wavelength at the lowest operated frequency in each design. The antenna in [1], [3], and [7] are more compact providing an omnidirectional pattern over the WLAN band; nonetheless, [1] and [7] offer a lower gain over 2.4/5 GHz WLAN, while [3] yields slightly higher gain covering only the lower band 2.4 GHz WLAN. The antenna structure in [2], [3], [5], [7], [9], [21] is more complicated. Table 2 shows that the proposed antenna possesses the same size as a small antenna in [5]-[9], [20], the simplest structure among 10 designs; meanwhile, it provides a kind of an omnidirectional pattern with good gain covering the 2.4/5 WLAN compared to other designs.

Table 2. Quality comparisons

Ref.	Antenna type	Dimension ( $\lambda_L$ )	Bandwidth	Pattern	Structure complexity	Gain (dBi)
[1]	3-D slots	0.18×0.08×0.20	2.38–2.51 GHz, 4.8–5.9 GHz	Omnidirectional	Less	1.6 2.3
[2]	8-array of a cavity and slot-dipole hybrid structure	$L \times 0.6L(N/A) \times 0.996$	2.39–2.49 GHz	Omnidirectional	More	10
[3]	Patch antenna	0.012×0.07×0.001	2.37–2.46 GHz	Quasi-omnidirectional	Medium	2.8
[5]	Filtenna	0.351×0.5×0.027	5.15–5.35 GHz	Omnidirectional	Medium	2.5
[6]	Franklin monopole	0.324×0.288×0.004	2.16–2.53 GHz, 4.58–5.8 GHz, 26.8–30 GHz	Nearly omnidirectional	More	1.95 3.76 7.35
[7]	3-sector loop-slot with stub and CMC	0.025×0.027×N/A	2.15–2.65 GHz, 4.85–5.92 GHz	Omnidirectional	Medium	0.95 2.43
[9]	DGS slots double-patch	0.35×0.35×0.004	2.45–2.495 GHz, 5.0–6.3 GHz, 23–28 GHz	Omnidirectional	More	3.55 4.72 5.85
[20]	Metamaterial	0.31×0.403×0.016	2.164–2.638 GHz, 4.48–5.812 GHz	Directional	Less	3.5 3.53
[21]	MIMO	0.9×0.375×0.005	2.25–2.63 GHz, 5.14–6.06 GHz	Unidirectional	More	5.2 6.7
This work	Pach with slots	0.384×0.304×0.013	2.4–2.8 GHz, 4.96–5.86 GHz	Omnidirectional	Less	2.55 3.3

#### 4. CONCLUSION

A dual-band patch antenna fabricated by a rectangular shape incorporated into a circular patch with a pair of inverted U-slots covering 2.4–2.8 GHz and 4.96–5.86 GHz to support 2.4/5 GHz WLAN applications is introduced. The proposed antenna is printed on the copper layer of the FR4 substrate, backed by a partial ground plane at the bottom layer, fed by a 50-Ohm microstrip line, and adjoined to the coaxial line via the subminiature version A connector. In this work, a pair of HWIUSs is crucial in breaking wideband to a two-bandwidth operation. The measured radiation pattern of the proposed DBPA shows the maximum gain of 2.55 dBi at 2.5 GHz and 3.3 dBi at 5.1 GHz, for linear polarization on its principal cut plane. The experimental  $|S_{11}|$ , normalized 2D-radiation pattern, and antenna gain affirm well simulation results. This antenna features a simple structure and radiating omnidirectional radiation pattern, making it suitable for dual operation at 2.4/5 GHz WLAN for indoor and outdoor applications. This single DBPA could be developed into an antenna array to enhance its performance in future research. Additionally, the antenna is protected by a radome in practical settings, which introduces further considerations for its design and performance in the next phases of development. This research seeks to contribute to the evolving landscape of wireless communication by providing an efficient dual-band omnidirectional antenna solution. This development will support the current demands of WLAN systems and provide a foundation for future advancements in mobile internet, IoT connectivity, and other wireless technologies.

#### ACKNOWLEDGEMENTS

This research project is supported by Rajamangala University of Technology Isan (contract no. ENG6/67).

#### REFERENCES





- [1] J. Guo, H. Bai, A. Feng, Y. Liu, Y. Huang, and X. Zhang, "A Compact Dual-Band Slot Antenna with Horizontally Polarized Omnidirectional Radiation," *IEEE Antennas and Wireless Propagation Letters*, vol. 20, no. 7, pp. 1234–1238, Jul. 2021, doi: 10.1109/LAWP.2021.3076169.






- [2] Y. Zhang and Y. Li, "Scalable Omnidirectional Dual-Polarized Antenna Using Cavity and Slot-Dipole Hybrid Structure," *IEEE Transactions on Antennas and Propagation*, vol. 70, no. 6, pp. 4215–4223, Jun. 2022, doi: 10.1109/TAP.2021.3138552.
- [3] H. H. Ibrahim *et al.*, "Low Profile Monopole Meander Line Antenna for WLAN Applications," *Sensors*, vol. 22, no. 16, p. 6180, Aug. 2022, doi: 10.3390/s22166180.
- [4] D. Sánchez-Hernández, *Multiband integrated antennas for 4G terminals*. Artech House, 2008.
- [5] M. M. Hosain, S. Kumari, and A. K. Tiwary, "Compact filterna for WLAN applications," *Journal of Microwaves, Optoelectronics and Electromagnetic Applications*, vol. 18, no. 1, pp. 70–79, Mar. 2019, doi: 10.1590/2179-10742019v18i11220.
- [6] M. E. Yassin, H. A. Mohamed, E. A. F. Abdallah, and H. S. El-Hennawy, "Single-fed 4G/5G multiband 2.4/5.5/28 GHz antenna," *IET Microwaves, Antennas and Propagation*, vol. 13, no. 3, pp. 286–290, Feb. 2019, doi: 10.1049/iet-map.2018.5122.
- [7] W. Song, Z. Weng, Y.-C. Jiao, L. Wang, and H.-W. Yu, "Omnidirectional WLAN Antenna With Common-Mode Current Suppression," *IEEE Transactions on Antennas and Propagation*, vol. 69, no. 9, pp. 5980–5985, Sep. 2021, doi: 10.1109/TAP.2021.3076261.
- [8] M. H. Seko and F. S. Corraera, "Quad-band printed antenna for portable WLAN applications," *Journal of Microwaves, Optoelectronics and Electromagnetic Applications*, vol. 18, no. 2, pp. 173–183, Jun. 2019, doi: 10.1590/2179-10742019v18i21506.
- [9] Z. Khan, M. H. Memon, S. Ur Rahman, M. Sajjad, F. Lin, and L. Sun, "A single-fed multiband antenna for WLAN and 5G applications," *Sensors (Switzerland)*, vol. 20, no. 21, pp. 1–13, Nov. 2020, doi: 10.3390/s20216332.
- [10] A. A. Jabber, A. K. Jassim, and R. H. Thaher, "Compact reconfigurable PIFA antenna for wireless applications," *Telkomnika (Telecommunication Computing Electronics and Control)*, vol. 18, no. 2, pp. 595–602, Apr. 2020, doi: 10.12928/telkomnika.v18i2.13427.
- [11] A. Annou, S. Berhab, and F. Chebbara, "Metamaterial-fractal-defected ground structure concepts combining for highly miniaturized triple-band antenna design," *Journal of Microwaves, Optoelectronics and Electromagnetic Applications*, vol. 19, no. 4, pp. 522–541, Dec. 2020, doi: 10.1590/2179-10742020V19I4894.
- [12] Z. Patel and A. Sarvaiya, "Novel series fed dual band circular polarization antenna for navigational satellite system," *TELKOMNIKA (Telecommunication Computing Electronics and Control)*, vol. 20, no. 2, p. 252, Apr. 2022, doi: 10.12928/telkomnika.v20i2.23315.
- [13] L. Chang and H. Liu, "Low-Profile and Miniaturized Dual-Band Microstrip Patch Antenna for 5G Mobile Terminals," *IEEE Transactions on Antennas and Propagation*, vol. 70, no. 3, pp. 2328–2333, Mar. 2022, doi: 10.1109/TAP.2021.3118730.
- [14] P. H. Juan and S. W. Su, "EMC Hybrid Loop/Monopole LDS Antenna With Three-Sided Ground Walls for 2.4/5/6 GHz WLAN Operation," *IEEE Antennas and Wireless Propagation Letters*, vol. 22, no. 9, pp. 2200–2204, Sep. 2023, doi: 10.1109/LAWP.2023.3281457.
- [15] S. E. Didi, I. Halkhams, M. Fattah, Y. Balboul, S. Mazer, and M. El Bekkali, "Design of a 2×2 dual band 28/38 GHz MIMO antenna in millimeter band for 5G," *Telkomnika (Telecommunication Computing Electronics and Control)*, vol. 22, no. 2, pp. 273–281, Apr. 2024, doi: 10.12928/TELKOMNIKA.v22i2.25268.
- [16] P. S. B. Ghose *et al.*, "A Compact Dual-Band Millimeter Wave Antenna for Smartwatch and IoT Applications with Link Budget Estimation," *Sensors*, vol. 24, no. 1, p. 103, Dec. 2023, doi: 10.3390/s24010103.
- [17] J. Li, J. Li, J. Yin, C. Guo, H. Zhai, and Z. Zhao, "A Miniaturized Dual-Band Dual-Polarized Base Station Antenna Loaded With Duplex Baluns," *IEEE Antennas and Wireless Propagation Letters*, vol. 22, no. 7, pp. 1756–1760, Jul. 2023, doi: 10.1109/LAWP.2023.3262824.
- [18] X.-F. Li, Y.-L. Ban, Q. Sun, Y.-X. Che, J. Hu, and Z. Nie, "A Compact Dual-Band Van Atta Array Based on the Single-Port Single-Band/Dual-Band Antennas," *IEEE Antennas and Wireless Propagation Letters*, vol. 22, no. 4, pp. 888–892, Apr. 2023, doi: 10.1109/LAWP.2022.3227577.
- [19] S. Lamultree, "Gain Improvement of Dual-Band Circular Monopole Antenna for 2.45/5.5 GHz WLAN Applications," *Przegląd Elektrotechniczny*, vol. 1, no. 5, pp. 159–162, May 2019, doi: 10.15199/48.2019.05.37.
- [20] X. Wu, X. Wen, J. Yang, S. Yang, and J. Xu, "Metamaterial Structure Based Dual-Band Antenna for WLAN," *IEEE Photonics Journal*, vol. 14, no. 2, 2022, doi: 10.1109/JPHOT.2022.3163170.
- [21] W. Zhang, Y. Li, K. Wei, and Z. Zhang, "A Dual-Band MIMO Antenna System for 2.4/5 GHz WLAN Applications," *IEEE Transactions on Antennas and Propagation*, vol. 71, no. 7, pp. 5749–5758, Jul. 2023, doi: 10.1109/TAP.2023.3277208.
- [22] X. Chen, J. Wang, and L. Chang, "Extremely Low-Profile Dual-Band Microstrip Patch Antenna Using Electric Coupling for 5G Mobile Terminal Applications," *IEEE Transactions on Antennas and Propagation*, vol. 71, no. 2, pp. 1895–1900, 2023, doi: 10.1109/TAP.2022.3217640.
- [23] Computer Simulation Technology, "Microwave Studio," *Research Base*, 2016. [Online]. Available: <https://sigmasolutions.co.th/en/cst-studio-suite>
- [24] G. Kumar and K. Ray, *Broadband microstrip antennas*. London: Institution of Engineering and Technology, 2013.
- [25] C. A. Balanis, "Antenna Theory: Analysis and Design 4th ed (Chapter2)," *SpringerReference*, no. 3, 2016.

## BIOGRAPHIES OF AUTHORS






**Suthasinee Lamultree**     received the B.Eng., and M.Eng., in Telecommunication Engineering from King Mongkut's Institute of Technology Ladkrabang, Thailand, in 2000 and 2003, respectively. In 2009, she received her D.Eng. in Electrical Engineering from the same institute. In 2016, she joined the Department of Electronics and Telecommunication Engineering, Faculty of Engineering, Rajamangala University of Technology Isan Khonkaen Campus, Khonkaen, Thailand. Her research interests include antenna design, microwave technology, and wireless communication systems. She can be contacted at email: [suthasinee.la@rmuti.ac.th](mailto:suthasinee.la@rmuti.ac.th).



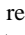


**Nattakarn Somsanook**    received the B.Eng. in Electronics and Telecommunication Engineering from the Faculty of Engineering, Rajamangala University of Technology Isan Khonkaen Campus, Thailand, in 2022. His research interests include antenna and circuit design. He can be contacted at email: [nattakarn.so@rmuti.ac.th](mailto:nattakarn.so@rmuti.ac.th).



**Wararak Narkkoht**    received the B.Eng. in Electronics and Telecommunication Engineering from the Faculty of Engineering, Rajamangala University of Technology Isan Khonkaen Campus, Thailand, in 2022. Her research interests include antenna and circuit design. She can be contacted at email: [wararak.na@rmuti.ac.th](mailto:wararak.na@rmuti.ac.th).



**Chuwong Phongcharoenpanich**    received his B.Eng. (Hons.), M.Eng., and D.Eng. degrees from King Mongkut's Institute of Technology Ladkrabang (KMITL), Bangkok, Thailand, in 1996, 1998, and 2001, respectively. Currently, he is the Professor of telecommunication engineering at the Department of Telecommunications Engineering, KMITL. He also serves as the head of the Innovative Antenna and Electromagnetic Applications Research Laboratory. His research interests are antenna design for various mobile and wireless communication devices, conformal antenna, and array antenna theory. He can be contacted at email: [chuwong.ph@kmitl.ac.th](mailto:chuwong.ph@kmitl.ac.th).